Preprint
UCRL-JC-149928

Beam Physics in X-ray Radiography Facilities

Yu-Jiuan Chen, G. J. Caporaso, F. W. Chambers, S. Falabella, F. J. Goldin, G.Guethlein, E. L. Lauer, J. F. McCarrick, R. Neurath, R. A. Richardson, S. Sampayan and J. T. Weir

This article was submitted to
Recent Progress in Induction Accelerator Workshop
Tsukuba, Japan, October 29-31,2002

December 2, 2002

BEAM PHYSICS IN X-RAY RADIOGRAPHY FACILITIES

Yu-Jiuan Chen, G. J. Caporaso, F. W. Chambers, S. Falabella, F. J. Goldin,
G. Guethlein, E. L. Lauer, J. F. McCarrick, R. Neurath, R. A. Richardson, S. Sampayan, and J. T. Weir
LLNL, Livermore, CA 94550, USA

Abstract

Performance of x-ray radiography facilities requires focusing the electron beams to sub-millimeter spots on the x-ray converters. Ions extracted from a converter by impact of a high intensity beam can partially neutralize the beam space charge and change the final focusing system. We will discuss these ion effects and mitigation.

1 INTRODUCTION

An ideal facility for flash x-ray radiography would provide multiple lines of sight to collect three-dimensional information on the object and would provide multiple high intensity x-ray pulses in time to take snapshots of temporal behavior. To achieve good resolution, the x-ray pulses' time integrated spot sizes need to be on the order of 1 mm. For example, the Dual Axis Radiographic Hydrodynamic Test facility (DARHT) is the first U. S. facility towards the ideal one. The first axis of DARHT (DARHT-I) is a single pulse machine, and the second axis of DARHT (DARHT-II) [1], [2] will deliver multiple electron pulses to a converter target. The performance specifications require the x-ray spot sizes to be no greater than ≤ 2.1 mm throughout the entire current pulse.

Several effects may impact the spot size. In a multiple pulsing machine, target plasma created by preceding current pulses can neutralize the beam space charge and change the focusing system. Interactions between the high intensity and high current beam and target plasma may also lead to instability. Fortunately, we can design the x-ray converter target so that hydro-expansion of target plasma into the incoming beam is minimized [3], [4], [5]. Thus, the spot size changes from pulse to pulse due to the charge neutralization effects of the target plasma are small. However, the time varying focusing forces of backstreaming ions pulled from the desorbed gas at the target surface in both a single-pulse machine and a multiple-pulse machine [6], or from a pre-existing target plasma plume in a multiple pulse machine by the electron beam's strong electric field may drastically change the spot size. We will not discuss how to design an x-ray converter target and the beam-plasma interaction in this paper. Only the backstreaming ion issues are discussed here.

We have investigated backstreaming ion emission and mitigation both computationally and experimentally. Comparison between PIC simulation results and the available experimental data indicates that if a mix of species is available, protons dominate the backstreaming ion effect, and that ion emission may be source limited. We have demonstrated experimentally that backstreaming ion effects can be minimized by pre-cleaning target surfaces with an electron beam or a laser. Confining the backstreaming ions within a short ion channel with a grounded foil-barrier to minimize their focusing effects on the e-beam's final spot size was first suggested by Hughes [6]. We have investigated the foil-barrier scheme experimentally and computationally as well; the results will be discussed in this paper. We will also discuss how the tuning strategy for beam transport affects the foil-barrier scheme's performance.

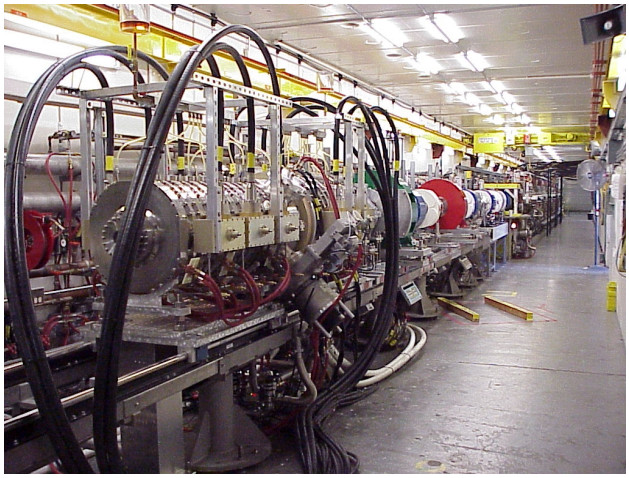

Fig. 1 THE ETA-II/SNOWTRON double pulse facility.

2 DOUBLE PULSE FACILITIES

We have been utilizing the ETA-II and SNOWTRON facilities at LLNL for the multi-pulsing, high x-ray dose converter target development activities [8]. These two machines are arranged to face each other as shown in Fig. 1 with the SNOWTRON injector in the foreground. The beams from both machines can be focused on to the same converter target with spot sizes about a millimeter FWHM. We have performed double-pulses experiments by firing the 1-MeV, 2-kA and 70-ns FWHM SNOWTRON beam to a converter target to create target plasma first, and firing the 6-MeV, 2-kA and 60-ns FWHM ETA-II beam to the same target several hundred naroseconds to a few microseconds later to characterize the beam-target interactions. With the double pulse setup, we have studied ion emission rate, gas desorption threshold temperature, foil barrier scheme and surface cleaning with e-beam & laser. With the ETA-II alone, we have also performed

target experiments to study ion emission rate and the foil barrier scheme.

3 IONS AND X-RAY DOSE

Depending on the ETA-II beam's incoming envelope, the spot disruption on the 6–MeV, 2-kA ETA-II beam due to the backstreaming ions could be weak during its flattop without a pre-existing plasma created on the target surface. To ensure that we simulate the DARHT-II beam-target interactions, backstreaming ion emission and surface cleaning, a double-pulse experiment was performed. Typically five diagnostics were taken for each shot. Backstreaming ions were collected by a Faraday cup at the ETA-II side. On-axis x-ray dose generated by the ETA-II beam was measured through a pair of apertures along a path that included the SNOWTRON cathode. The ETA-II x-ray spots at 10 ns before and 15 ns after the center of the flattop were recorded by imaging the optical transition radiation from the target. The time integrated SNOWTRON beam spot was taken by an optical framing camera.

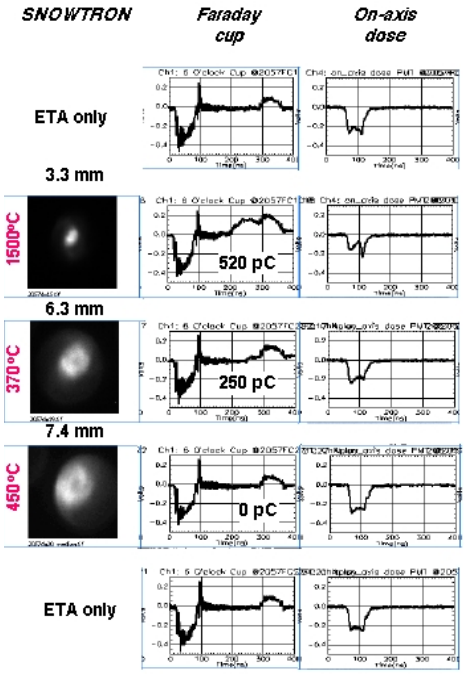

Figure 2. The SNOWTRON beam images with beam sizes, estimated graphite temperatures, the Faraday cup's ion signals, and the forward on-axis x-ray doses generated by the ETA-II beam for the ETA-II/SNOWTRON double-pulse experiment.

Figure 2 demonstrates how ion emission from a 3-mil graphite foil affects the forward x-ray production. The separation between the SNOWTRON beam and the ETA-II beam was 2 μs for this set of data. The first column presents the SNOWTRON beam images if the SNOWTRON was fired. The second column presents the ion signals detected by Faraday cup. The total ion charge collected by the cup is also shown with each Faraday cup data. The third column gives the on-axis x-ray doses generated by the ETA-II beam. The first and the last rows present the nominal data when the SNOWTRON beam was not fired. With the specific EAT-II beam envelope used for the experiment, no ion signals were detected by the Faraday cup, which indicate that the backstreaming ion effects were weak. Rows 2-4 present data for various SNOWTRON spot sizes. The calculated peak foil temperature based on energy deposition is given at the side of each row. Comparing Rows 3 and 4 suggests that ion emission due to gas desorption occurs around 400ºC, which agrees with observations on ion emission in an IVA diode reported in Ref. [9]. Figure 2 clearly shows that the backstreaming ions cause reduction of the forward x-ray dose.

4 ION EMISSION

Concerning that ions desorbed from solid surfaces by an incoming DARHT-II beam (18.6 MeV, 2 kA and 2μs) would upset the transport system. The LANL DARHT group performed a double foil experiment [10] at the 19.8 MeV, 2-kA DARHT-I facility to study these ion focusing effects. The beam was focused onto a thin foil of various materials to minimize the beam scattering. The ions generated by the beam moved both upstream and downstream to form ion channels on the both sides of the foil. The ion focusing effects were then observed by measuring the time-varying beam radius on a witness foil 65 cm downstream. They had observed beam spot size disruption and a transverse beam instability at the witness foil. These data can generally be explained with ionization of water vapor on the foil surface. By assuming that 91% of ions are H_2O^+, OH^+, O^+ and the remaining are H^+, and extrapolating the impact ionization data for 10 - 1 kV electrons to 20 MeV electrons, their PIC simulations of space charge limited emission of the mixture yield to 40% of the current in protons. The simulated beam disruption with an Al foil matches the experimental data very well. Frequency of the instability also suggests that the main species in the ion channel was protons. It is interesting to note that they did not observe any spot size disruption on all types of target foils even for a small beam spot (1.5 - 2.5 mm FWHM) both computational and experimentally, which may indicate that the backstreaming ion effect may not be an issue for 20-MeV single pulse x-ray radiography facilities.

We have performed a similar experiment [11], [12], with similar sensitivities and similar deposited energy densities on some of the same types of materials, at the 6-MeV, 2-kA ETA-II facility. One material used as a target foil in the ETA-II experiment but not in the DARHT-I experiment is quartz. The ETA-II beam impinging on the dielectric quartz surface created flashover and a rich ion source for space charge limited emission at t = 0. Figure 3 shows the ETA-II temporal FWHM beam size on the witness foil when flashover occurred on the quartz foil.

Two experimental data for two magnetic settings are shown in (a). Simulated temporal beam size with space-charge-limited emission for H^+ and for C^+ from t =0 are shown in (b) and (c), respectively. The match between the data and the simulated H^+ emission case is quite good. The simulated profiles do not match the data when other heavier ions are used in the simulations (see Fig.1c). These comparisons suggest that if a mix of species is available, protons may dominate the backstreaming ion effects; however, simulations where multiple species are available have not been done, as this requires more sophisticated modelling of the emission sheath. Given the quality of the match and lacking any direct measurements of the emitted species, all the simulations presented later in this paper assume only protons emitted from a surface.

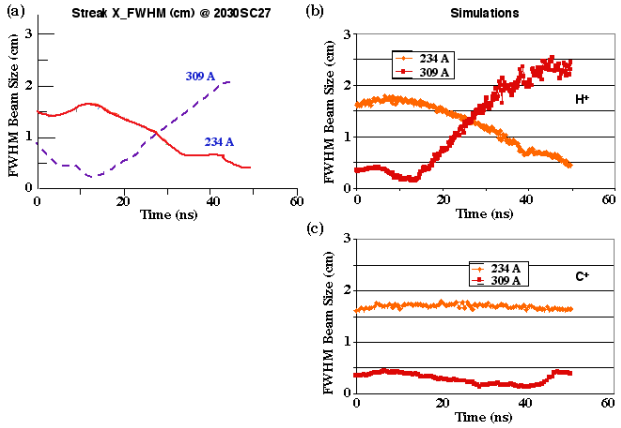

Figure 3. The ETA-II temporal FWHM beam size on the witness foil when flashover occurred on the quartz foil. Two experimental data for two magnetic settings are shown in (a). Simulated temporal beam size with space-charge-limited emission for H^+ and for C^+ are shown in (b) and (c), respectively.

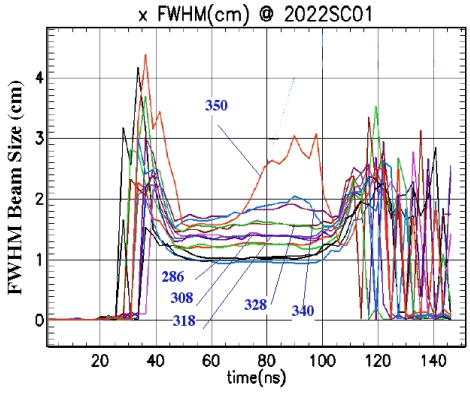

Figure 4. Beam spot temporal behaviors in the ETA-II double foil experiments. The foil used to obtain the ETA-II data was aluminum.

According to Ref. [10], the DARHT data indicate that there was a source of ions even at relatively low temperatures. Based on their beam disruption rates, the strongest effects on the DARHT-I beam were seen with Ta and Ti foils. However, the beam disruption was observed on the ETA-II only when the impact of the beam turned the target foil to plasma or when a quartz foil was used as the target foil and there was flashover on the quartz surface. Otherwise, the ETA-II data did not show any observable ion emission effects over error bars within the flattop top for beam radius less than 2 mm as shown in Fig. 4. An Al foil was used as the target foil for this data set. PIC simulations assuming the space charge limited emission conditions for various species do not match either the DARHT-I or the ETA-II experiment. The resulting beam disruption would occur much sooner and be much stronger than what is observed on DARHT-I. Models using a delayed onset of space charge limited emission until the barrier material reaches a threshold temperature can match the onset time but not the rate of beam disruption. In order to reconcile the results, an ion emission model [12], [13] that provides two free parameters, the bounding energy between the absorbed gas and the foil material and the surface density of the desorbed neutral, has been incorporated into the PIC simulations. The binding energy determines the onset time of beam disruption, and the surface density determines the beam disruption rate.

Consider a subset of the DARHT-I data consisting of the first 50 ns of the flattop and compare it to the flattop data from ETA-II (see Fig. 2). Since the curves for Ta and Ti are not available for ETA-II, it becomes clear that 50 ns is not long enough to resolve the ion effect above the error bars of the ETA-II data. Thus the experimental data can be matched by adjusting the binding energy to produce an onset later than would be resolved on ETA-II, and then adjusting the surface density of the desorbed neutral to produce the correct slope of the DARHT-I data thereafter. Figure 6 shows the results of a simulation assuming a binding energy of 0.47 eV and 3 monolayers of adsorbed gas compared with the 70 ns flattop of the DARHT-I data (with the Ta and Ti curves removed).

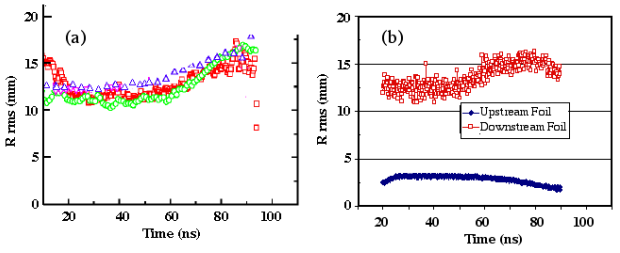

Figure 5. Comparison of the temporal beam sizes over 70 ns flattop from the DARHT-I double-foil experiment (left) and from the simulation using the gas desorption / ionization model and assuming 3 monolayers of adsorbed gas and a binding energy of 0.47 eV (right).

As mentioned earlier, the simulations presented here only involve one species of ions, namely protons. However, the resulted proton current is similar to what

was obtained from the simulations in Ref. [10] with space charge limited emission of multiple species from ionized water vapor; and it can match both the rapid DARHT-I beam disruption shown in Fig. 5 and the slow disruption shown in Fig. 4. Hence, we believe that although the simple model glosses over the mix of physics giving rise to gas desorption, it does serve to reconcile the available experimental data and gives a rough quantification of emission current, showing that it is source limited. It is then possible that surface cleaning will be sufficient to avoid this type of emission from the barrier surface.

5 MITIGATION

5.1 Surface cleaning

We have investigated two methods of surface cleaning. We have first studied cleaning the surface of a graphite foil with a SNOWTRON beam. The SNOWTRON beam was used to create target plasma as discussed in Sec. 3. However, to pre-clean the surface, SNOWTRON was fired twice with a 1-second separation. The SNOWTRON beam spot sizes were 3.3 mm FWHM for both plasma creation and surface cleaning. The estimated graphite temperature is 1500°C for both cases shown in Fig. 6. Without pre-cleaning (shown in Fig. 6a), more ions were detected by Faraday cup. The ETA-II beam spot was spoiled, and the on-axis x-ray dose was reduced. With a pre-cleaning beam pulse, the Faraday cup signal in Fig. 6b indicates that the first pulse cleaned the foil surface and reduced ion emission. Hence, e-beam cleaning preserved the beam spot size and on-axis x-ray dose.

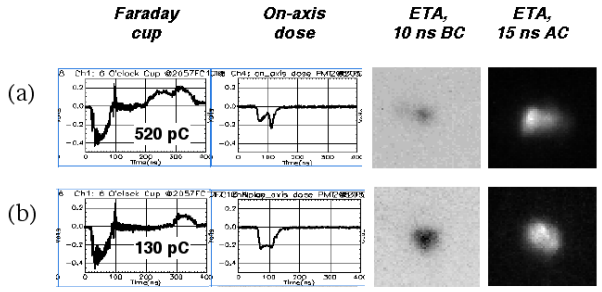

Figure 6. The ion signals, forward axial x-ray doses generated by the ETA-II beam and ETA-II beam images for the e-beam cleaning experiment with a 3.3 mm SNOWTRON spot size.

We have also investigated using a pulsed laser to pre-clean graphite foil. A 6-mil graphite foil, which was backed with a 10-mil quartz foil serving as a Cherenkov witness foil, was used as a target. A 60-mJ Nd:YAG laser at 1.06 μm was used to pre-clean the graphite. Since the backstreaming ions' spot size disruption effects on the ETA-II beam is weak without a pre-existing plasma, the laser was also used to create plasma on the graphite foil surface at 2 μs before the ETA-II beam was fired. The separation between the plasma generating laser pulse and the onset of the cleaning pulse train is 1 second. As shown in Fig. 7, without pre-cleaning, the beam blew up rapidly in the presence of ions and formed a large halo. The image of the halo is barely visible because the x-ray intensity created by the halo was small. The laser spot used for pre-cleaning and e-beam disruption was about 5 mm in diameter. Figure 7 also shows that the ETA-II spot was preserved effectively through the entire beam flattop if 100 laser pulses were fired onto the same spot on the foil. Presumably those laser pulses have cleaned the graphite surface.

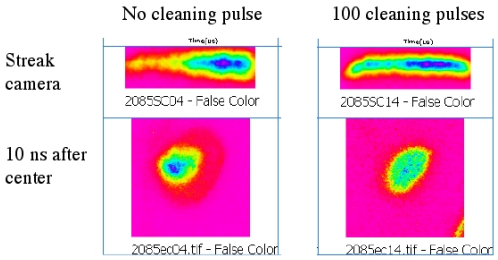

FIGURE 7. The ETA-II beam spot sizes with and without 100 cleaning laser pulses.

5.2 Foil barrier

Confining the backstreaming ions within a short ion channel with a grounded foil-barrier to minimize their focusing effects on the e-beam's final spot size was investigated. Effectiveness of the foil-barrier scheme was demonstrated [14] on the ETA-II/SNOWTRON double pulse facility. The time varying x-ray spot sizes created by the ETA-II beam for this study were shown in Fig. 8. The weak backstreaming ion effects on the ETA-II beam without pre-existing plasma are demonstrated by the small variation in beam spot sizes in the left column. The central column shows that when plasma was created by the SNOWTRON beam 600 ns prior to the ETA pulse, the focus of the ETA-II beam was destroyed within 20 ns if a foil-barrier was not used. However, if a grounded foil was placed 1 cm in front of the ETA-II side of the target, the spot size was preserved through the entire ETA-II flattop (shown in the right column).

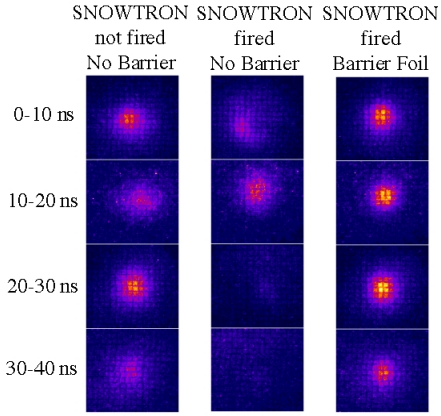

Figure 8. The x-ray spot sizes on the ETA-II/ SNOWTRON double-pulse foil-barrier experiment.

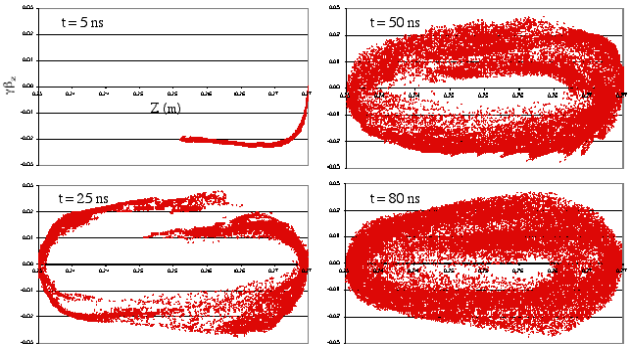

Figure 9. Snapshots of the z-$\gamma\beta_z$ ion phase space obtained from a PIC simulation of the nominal DARHT-II target/barrier system.

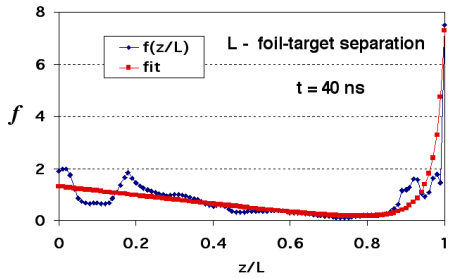

Figure 10. The neutralization fraction f within the nominal DARHT-II target/barrier system. The normalized target location is 1, and the barrier is located at 0.

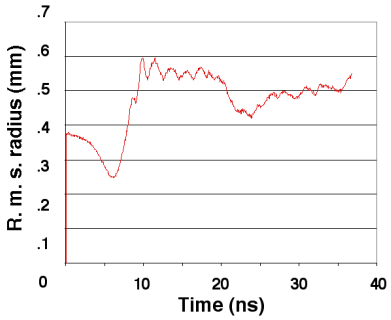

Figure 11. Temporal behaviors of beam spot size on the target, as r.m.s. value in the X plane in a baseline DARHT-II target/barrier system.

While the use of a grounded foil to stop backstreaming ions has been successful on the ETA-II, there are several concerns regarding how to implement the foil-barrier scheme effectively. The region between the grounded foil-barrier and the grounded target surface serves as an ion trap. As shown in Fig. 9 and discussed in Ref. [12], although the backstreaming ions reach the foil-barrier within only a few nanoseconds, the time for ions filling up the trap is longer than the beam pulse length. While the asymptotic result of using a foil-barrier is that ion charge accumulates between the target and barrier, and moves towards a steady-state configuration of complete neutralization of the electron beam, there are no ions (i.e., a neutralization fraction, f, of 0) at the start of a beam pulse, and the system evolves with time towards f = 1. The spatial profile of the neutralization evolves as well (see Fig. 10). The scaling law for the ion channel's disruption length L_D [15] is given as $L_D \cong (\pi\gamma\beta^2 I_o/fI)^{1/2}a$, where I and I_o is the beam current and Alfven current, respectively, and a is the beam radius. This scaling law indicates that the suitable foil-target separation depends on the overall beam envelope inside the ion trap region and ions' neutralization fraction. The long fill time of the trap and the transient behavior of the neutralization fraction may not lend themselves to a "clean" performance of the target system from a radiographic standpoint. As shown in Fig. 11, while the foil barrier scheme does minimize beam disruption reasonably well, the time integrated spot size is better preserved for a long pulse beam than for a short pulse beam. Potentially, we can reduce the transient behavior of the ion trap by placing the foil closely to the target for a single pulse machine. However, the spot size on a closely placed foil will be too small to be practical for a multi-pulse machine since the foil may not survive the impact of multiple beam pulses.

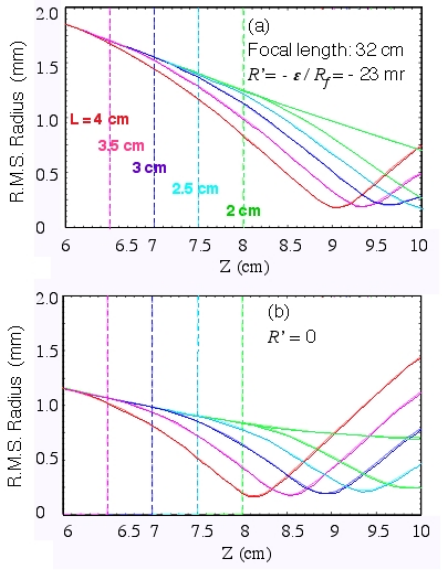

Figure 12. The r.m.s. beam envelopes in the foil-barrier traps with various foil-target separations

Instead of shortening the foil-target separation, the foil-barrier's performance can also be improved by using a different focusing scheme to obtain a larger beam envelope, i.e., a larger envelope convergence, in the ion trap region without sacrificing the final spot size. As demonstrated by Fig. 12, this results in weaker ion focusing forces, which reduces sensitivity of the final beam spot size to small beam envelope variation, and a larger beam spot on the foil, which is preferable for foil survivability. Figure 12 shows the r.m.s. beam envelopes (curves) with a foil (vertical dashes) placed at 4, 3.5, 3, 2.5, 2 or 0 cm in front of the target surface. The beam is focused beyond the target front surface in Fig. 12a and on the front surface in Fig. 12b. The focusing scheme used

for Fig. 12a is better for a multi-pulse machine since the foil can be placed further upstream from the target, and hence, the beam size on the foil is larger for better foil survivability. Comparison between the envelope curve corresponding to a 4-cm separation in Fig. 12a and that corresponding to a 3-cm separation in Fig. 12b indicates that the final beam spot sizes and the resulting beam divergence are also similar. Hence, the final x-ray spot sizes and forward x-ray doses are similar for these two cases if the emittance growth due to foil scattering does not dominate the final beam emittance. However, if the emittance growth due to foil scattering is significant, opening up the beam envelope in the ion trap region would cause noticeable x-ray dose reduction. The final concern regarding the foil-barrier scheme is that the nonlinear ion forces in the ion trap may also cause large emittance growth, which again leads to dose reduction.

6 SUMMARY

Performance of x-ray radiography facilities requires focusing the electron beams to sub-millimeter spots on the x-ray converters. It is a concern that ions desorbed from x-ray converter target by an incoming high intensity, high current electron beam, and subsequently accelerated and trapped by the beam space charge potential, will provide unwanted charge neutralization to the beam, upsetting the transport system. While the mechanisms of ion emission from either a solid target surface or target plasma are still not understood, ion emission can be minimized by cleaning the surface with an electron beam or several laser pulses. The unwanted ion focusing effects can also be minimized by using a grounded foil to trap ions in a small region. However, the beam radius will exhibit some transient behavior due to the trapped ions' long fill time in the longitudinal phase space. The foil-barrier's performance in terms of spot size sensitivity to beam parameters and foil survivability can be improved by using a focusing scheme, which provides a large beam envelope with a fast convergence in the trap region. However, a faster converging beam means a larger spot size on the foil-barrier, and hence, a larger emittance growth caused by foil scattering, which may lead to unacceptable x-ray dose reduction.

7 ACKNOWLEDGMENTS

This work was performed under the auspices of the U.S. Department of Energy by University of California Lawrence Livermore National Laboratory under contract No. W-7405-Eng-48.

8 REFERENCES

[1] M. J. Burns, et al., "Status of the DARHT Phase 2 Long-Pulse Accelerator", *Proceedings of the 2001 Particle Accelerator Conference*, Chicago, Illinois, 2001, pp. 325-329.

[2] M. J. Burns, et al., "Status of the Dual Axis Radiographic Hydrodynamics Test (DARHT) Facility", *Proceedings of the 14th High-Power Particle Beams*, Albuquerque, New Mexico, 2002.

[3] P. A. Pincosy, et al., "Multiple pulse electron beam converter design for high power radiography", *Review of Scientific Instruments*, **72,** 2599-2604 (2001).

[4] D. D.-M. Ho, et al., "Hydrodynamic Modeling of a Multi-Pulse X-Ray Converter Target for DARHT-II", LLNL Report No. UCRL-JC-1442, July 26, 2001.

[5] Y.-J. Chen, et al., "Downstream System for the Second Axis of the DARHT Facility", *Proceedings of the XXI LINAC*, Gyeongju, Korea, Aug. 19-23, 2002.

[6] D. R. Welch and T. P. Hughes, Laser Part. Beams **16**, 285-294 (1998).

[7] T. P. Hughes, "Target Calculations for ITS Short-Focus Experiment", MRC/ABQ-N-589, September 1997.

[8] Y.-J. Chen, et. al., "Physics Design of the ETA-II/Snowtron Double Pulse Target Experiment", *XX International LINAC Conference*, Monterey, California, 2000, pp. 482-484.

[9] Sanford, T. W. L., et al., *J. appl. Phys.* **66,** 10-22 (1989).

[10] H. A. Davis, et al., to be published by *Physics of Plasma*, 2002.

[11] E. L. Lauer, et al., "Search for Backstreaming Ion Defocusing Using A Single Pulse of a 2 kA Relativistic electron Beam." *Proceedings of the 14th International Conference on High-Power Particle Beams*, Albuquerque, New Mexico, 2002.

[12] Y.-J. Chen, et al., "High Intensity Beam and X-Ray Converter Target Interactions and Mitigation", *Proceedings of the Advanced Accelerator Concept Workshop*, Oxnard, CA, 2002.

[13] B. V. Oliver, et al., "Beam-Target Interactions in Single- and Multi-Pulse Radiography." Report MRC/ABQ-R-1909, Mission Research Corporation, Albuquerque, New Mexico, 1999.

[14] S. Sampayan, et. al., "Beam-Target Interaction Experiments for Multipulse Bremsstrahlung Converters Applications", *Proceedings of the 2001 Particle Accelerator Conference*, Chicago, Illinois, 2001, pp. 330-332.

[15] Caporaso, G. J. and Chen, Y.-J., *Proc. of the XIX LINAC Conference*, Chicago, Illinois, 1998, pp. 831-833.